N·H

ELSEVIER

Search for charginos, neutralinos and gravitinos in e^+e^- interactions at $\sqrt{s} = 183$ GeV

DELPHI Collaboration

P. Abreu [u], W. Adam [ax], T. Adye [aj], P. Adzic [k], I. Ajinenko [ap], T. Aldeweireld [b],
G.D. Alekseev [p], R. Alemany [aw], T. Allmendinger [q], P.P. Allport [v], S. Almehed [x],
U. Amaldi [i], S. Amato [au], E.G. Anassontzis [c], P. Andersson [ar], A. Andreazza [i],
S. Andringa [u], P. Antilogus [y], W-D. Apel [q], Y. Arnoud [n], B. Åsman [ar],
J-E. Augustin [y], A. Augustinus [i], P. Baillon [i], P. Bambade [s], F. Barao [u],
G. Barbiellini [at], R. Barbier [y], D.Y. Bardin [p], G. Barker [i], A. Baroncelli [al],
M. Battaglia [o], M. Baubillier [w], K-H. Becks [az], M. Begalli [f], P. Beilliere [h],
Yu. Belokopytov [i,1], A.C. Benvenuti [e], C. Berat [n], M. Berggren [y], D. Bertini [y],
D. Bertrand [b], M. Besancon [am], F. Bianchi [as], M. Bigi [as], M.S. Bilenky [p],
M-A. Bizouard [s], D. Bloch [j], H.M. Blom [ad], M. Bonesini [aa], W. Bonivento [aa],
M. Boonekamp [am], P.S.L. Booth [v], A.W. Borgland [d], G. Borisov [s], C. Bosio [ao],
O. Botner [av], E. Boudinov [ad], B. Bouquet [s], C. Bourdarios [s], T.J.V. Bowcock [v],
I. Boyko [p], I. Bozovic [k], M. Bozzo [m], P. Branchini [al], T. Brenke [az], R.A. Brenner [av],
P. Bruckman [r], J-M. Brunet [h], L. Bugge [af], T. Buran [af], T. Burgsmueller [az],
P. Buschmann [az], S. Cabrera [aw], M. Caccia [aa], M. Calvi [aa], A.J. Camacho Rozas [an],
T. Camporesi [i], V. Canale [ak], F. Carena [i], L. Carroll [v], C. Caso [m],
M.V. Castillo Gimenez [aw], A. Cattai [i], F.R. Cavallo [e], V. Chabaud [i],
Ph. Charpentier [i], L. Chaussard [y], P. Checchia [ai], G.A. Chelkov [p], R. Chierici [as],
P. Chliapnikov [ap], P. Chochula [g], V. Chorowicz [y], J. Chudoba [ac], P. Collins [i],
R. Contri [m], E. Cortina [aw], G. Cosme [s], F. Cossutti [am], J-H. Cowell [v], H.B. Crawley [a],
D. Crennell [aj], G. Crosetti [m], J. Cuevas Maestro [ag], S. Czellar [o], G. Damgaard [ab],
M. Davenport [i], W. Da Silva [w], A. Deghorain [b], G. Della Ricca [at], P. Delpierre [z],
N. Demaria [i], A. De Angelis [i], W. De Boer [q], S. De Brabandere [b], C. De Clercq [b],
B. De Lotto [at], A. De Min [ai], L. De Paula [au], H. Dijkstra [i], L. Di Ciaccio [ak],
J. Dolbeau [h], K. Doroba [ay], M. Dracos [j], J. Drees [az], M. Dris [ae], A. Duperrin [y],
J-D. Durand [y,i], G. Eigen [d], T. Ekelof [av], G. Ekspong [ar], M. Ellert [av], M. Elsing [i],
J-P. Engel [j], B. Erzen [aq], M. Espirito Santo [u], E. Falk [x], G. Fanourakis [k],

D. Fassouliotis [k], J. Fayot [w], M. Feindt [q], P. Ferrari [aa], A. Ferrer [aw], E. Ferrer-Ribas [s],
S. Fichet [w], A. Firestone [a], P.-A. Fischer [i], U. Flagmeyer [az], H. Foeth [i], E. Fokitis [ae],
F. Fontanelli [m], B. Franek [aj], A.G. Frodesen [d], R. Fruhwirth [ax], F. Fulda-Quenzer [s],
J. Fuster [aw], A. Galloni [v], D. Gamba [as], S. Gamblin [s], M. Gandelman [au], C. Garcia [aw],
J. Garcia [an], C. Gaspar [i], M. Gaspar [au], U. Gasparini [ai], Ph. Gavillet [i], E.N. Gazis [ae],
D. Gele [j], L. Gerdyukov [ap], N. Ghodbane [y], I. Gil [aw], F. Glege [az], R. Gokieli [ay],
B. Golob [aq], G. Gomez-Ceballos [an], P. Goncalves [u], I. Gonzalez Caballero [an],
G. Gopal [aj], L. Gorn [a,2], M. Gorski [ay], Yu. Gouz [ap], V. Gracco [m], J. Grahl [a],
E. Graziani [al], C. Green [v], H-J. Grimm [q], P. Gris [am], K. Grzelak [ay], M. Gunther [av],
J. Guy [aj], F. Hahn [i], S. Hahn [az], S. Haider [i], A. Hallgren [av], K. Hamacher [az],
F.J. Harris [ah], V. Hedberg [x], S. Heising [q], J.J. Hernandez [aw], P. Herquet [b], H. Herr [i],
T.L. Hessing [ah], J.-M. Heuser [az], E. Higon [aw], S-O. Holmgren [ar], P.J. Holt [ah],
D. Holthuizen [ad], S. Hoorelbeke [b], M. Houlden [v], J. Hrubec [ax], K. Huet [b],
G.J. Hughes [v], K. Hultqvist [ar], J.N. Jackson [v], R. Jacobsson [i], P. Jalocha [i], R. Janik [g],
Ch. Jarlskog [x], G. Jarlskog [x], P. Jarry [am], B. Jean-Marie [s], E.K. Johansson [ar],
P. Jonsson [y], C. Joram [i], P. Juillot [j], F. Kapusta [w], K. Karafasoulis [k], S. Katsanevas [y],
E.C. Katsoufis [ae], R. Keranen [q], B.P. Kersevan [aq], B.A. Khomenko [p],
N.N. Khovanski [p], A. Kiiskinen [o], B. King [v], A. Kinvig [v], N.J. Kjaer [ad], O. Klapp [az],
H. Klein [i], P. Kluit [ad], P. Kokkinias [k], M. Koratzinos [i], V. Kostioukhine [ap],
C. Kourkoumelis [c], O. Kouznetsov [p], M. Krammer [ax], C. Kreuter [i], E. Kriznic [aq],
J. Krstic [k], Z. Krumstein [p], P. Kubinec [g], W. Kucewicz [r], J. Kurowska [ay],
K. Kurvinen [o], J.W. Lamsa [a], D.W. Lane [a], P. Langefeld [az], V. Lapin [ap],
J-P. Laugier [am], R. Lauhakangas [o], G. Leder [ax], F. Ledroit [n], V. Lefebure [b],
L. Leinonen [ar], A. Leisos [k], R. Leitner [ac], J. Lemonne [b], G. Lenzen [az], V. Lepeltier [s],
T. Lesiak [r], M. Lethuillier [am], J. Libby [ah], D. Liko [i], A. Lipniacka [ar], I. Lippi [ai],
B. Loerstad [x], J.G. Loken [ah], J.H. Lopes [au], J.M. Lopez [an], R. Lopez-Fernandez [n],
D. Loukas [k], P. Lutz [am], L. Lyons [ah], J.R. Mahon [f], A. Maio [u], A. Malek [az],
T.G.M. Malmgren [ar], V. Malychev [p], F. Mandl [ax], J. Marco [an], R. Marco [an],
B. Marechal [au], M. Margoni [ai], J-C. Marin [i], C. Mariotti [i], A. Markou [k],
C. Martinez-Rivero [s], F. Martinez-Vidal [aw], S. Marti i Garcia [i],
N. Mastroyiannopoulos [k], F. Matorras [an], C. Matteuzzi [aa], G. Matthiae [ak], J. Mazik [ac],
F. Mazzucato [ai], M. Mazzucato [ai], M. Mc Cubbin [v], R. Mc Kay [a], R. Mc Nulty [v],
G. Mc Pherson [v], C. Meroni [aa], W.T. Meyer [a], A. Miagkov [ap], E. Migliore [as],
L. Mirabito [y], W.A. Mitaroff [ax], U. Mjoernmark [x], T. Moa [ar], R. Moeller [ab],
K. Moenig [i], M.R. Monge [m], X. Moreau [w], P. Morettini [m], G. Morton [ah],
U. Mueller [az], K. Muenich [az], M. Mulders [ad], C. Mulet-Marquis [n], R. Muresan [x],
W.J. Murray [aj], B. Muryn [n,r], G. Myatt [ah], T. Myklebust [af], F. Naraghi [n],
F.L. Navarria [e], S. Navas [aw], K. Nawrocki [ay], P. Negri [aa], S. Nemecek [l], N. Neufeld [i],

N. Neumeister [ax], R. Nicolaidou [n], B.S. Nielsen [ab], M. Nikolenko [j,p],
V. Nomokonov [o], A. Normand [v], A. Nygren [x], V. Obraztsov [ap], A.G. Olshevski [p],
A. Onofre [u], R. Orava [o], G. Orazi [j], K. Osterberg [o], A. Ouraou [am], M. Paganoni [aa],
S. Paiano [e], R. Pain [w], R. Paiva [u], J. Palacios [ah], H. Palka [r], Th.D. Papadopoulou [ae],
K. Papageorgiou [k], L. Pape [i], C. Parkes [ah], F. Parodi [m], U. Parzefall [v], A. Passeri [al],
O. Passon [az], M. Pegoraro [ai], L. Peralta [u], M. Pernicka [ax], A. Perrotta [e], C. Petridou [at],
A. Petrolini [m], H.T. Phillips [aj], F. Pierre [am], M. Pimenta [u], E. Piotto [aa],
T. Podobnik [aq], M.E. Pol [f], G. Polok [r], P. Poropat [at], V. Pozdniakov [p], P. Privitera [ak],
N. Pukhaeva [p], A. Pullia [aa], D. Radojicic [ah], S. Ragazzi [aa], H. Rahmani [ae],
D. Rakoczy [ax], P.N. Ratoff [t], A.L. Read [af], P. Rebecchi [i], N.G. Redaelli [aa],
M. Regler [ax], D. Reid [i], R. Reinhardt [az], P.B. Renton [ah], L.K. Resvanis [c],
F. Richard [s], J. Ridky [l], G. Rinaudo [as], O. Rohne [af], A. Romero [as], P. Ronchese [ai],
E.I. Rosenberg [a], P. Rosinsky [g], P. Roudeau [s], T. Rovelli [e], Ch. Royon [am],
V. Ruhlmann-Kleider [am], A. Ruiz [an], H. Saarikko [o], Y. Sacquin [am], A. Sadovsky [p],
G. Sajot [n], J. Salt [aw], D. Sampsonidis [k], M. Sannino [m], H. Schneider [q],
Ph. Schwemling [w], U. Schwickerath [q], M.A.E. Schyns [az], F. Scuri [at], P. Seager [t],
Y. Sedykh [p], A.M. Segar [ah], R. Sekulin [aj], R.C. Shellard [f], A. Sheridan [v],
M. Siebel [az], L. Simard [am], F. Simonetto [ai], A.N. Sisakian [p], T.B. Skaali [af],
G. Smadja [y], O. Smirnova [x], G.R. Smith [aj], A. Sokolov [ap], O. Solovianov [ap],
A. Sopczak [q], R. Sosnowski [ay], T. Spassov [u], E. Spiriti [al], P. Sponholz [az],
S. Squarcia [m], D. Stampfer [ax], C. Stanescu [al], S. Stanic [aq], S. Stapnes [af],
K. Stevenson [ah], A. Stocchi [s], J. Strauss [ax], R. Strub [j], B. Stugu [d],
M. Szczekowski [ay], M. Szeptycka [ay], T. Tabarelli [aa], F. Tegenfeldt [av],
F. Terranova [aa], J. Thomas [ah], A. Tilquin [z], J. Timmermans [ad], N. Tinti [e],
L.G. Tkatchev [p], S. Todorova [j], D.Z. Toet [ad], B. Tome [u], A. Tonazzo [aa], L. Tortora [al],
G. Transtromer [x], D. Treille [i], G. Tristram [h], M. Trochimczuk [ay], C. Troncon [aa],
A. Tsirou [i], M-L. Turluer [am], I.A. Tyapkin [p], S. Tzamarias [k], B. Ueberschaer [az],
O. Ullaland [i], V. Uvarov [ap], G. Valenti [e], E. Vallazza [at], C. Vander Velde [b],
G.W. Van Apeldoorn [ad], P. Van Dam [ad], W.K. Van Doninck [b], J. Van Eldik [ad],
A. Van Lysebetten [b], I. Van Vulpen [ad], N. Vassilopoulos [ah], G. Vegni [aa],
L. Ventura [ai], W. Venus [aj], F. Verbeure [b], M. Verlato [ai], L.S. Vertogradov [p],
V. Verzi [ak], D. Vilanova [am], L. Vitale [at], E. Vlasov [ap], A.S. Vodopyanov [p],
C. Vollmer [q], G. Voulgaris [c], V. Vrba [l], H. Wahlen [az], C. Walck [ar], C. Weiser [q],
D. Wicke [az], J.H. Wickens [b], G.R. Wilkinson [i], M. Winter [j], M. Witek [r], G. Wolf [i],
J. Yi [a], O. Yushchenko [ap], A. Zalewska [r], P. Zalewski [ay], D. Zavrtanik [aq],
E. Zevgolatakos [k], N.I. Zimin [p,x], G.C. Zucchelli [ar], G. Zumerle [ai]

[a] *Department of Physics and Astronomy, Iowa State University, Ames, IA 50011-3160, USA*
[b] *Physics Department, Univ. Instelling Antwerpen, Universiteitsplein 1, BE-2610 Wilrijk, Belgium, and IIHE, ULB-VUB, Pleinlaan 2,
BE-1050 Brussels, Belgium, and Faculté des Sciences, Univ. de l'Etat Mons, Av. Maistriau 19, BE-7000 Mons, Belgium*

[c] *Physics Laboratory, University of Athens, Solonos Str. 104, GR-10680 Athens, Greece*
[d] *Department of Physics, University of Bergen, Allégaten 55, NO-5007 Bergen, Norway*
[e] *Dipartimento di Fisica, Università di Bologna and INFN, Via Irnerio 46, IT-40126 Bologna, Italy*
[f] *Centro Brasileiro de Pesquisas Físicas, rua Xavier Sigaud 150, BR-22290 Rio de Janeiro, Brazil, and Depto. de Física, Pont. Univ. Católica, C.P. 38071 BR-22453 Rio de Janeiro, Brazil, and Inst. de Física, Univ. Estadual do Rio de Janeiro, rua São Francisco Xavier 524, Rio de Janeiro, Brazil*
[g] *Comenius University, Faculty of Mathematics and Physics, Mlynska Dolina, SK-84215 Bratislava, Slovakia*
[h] *Collège de France, Lab. de Physique Corpuscolaire, IN2P3-CNRS, FR-75231 Paris Cedex 05, France*
[i] *CERN, CH-1211 Geneva 23, Switzerland*
[j] *Institut de Recherches Subatomiques, IN2P3 - CNRS / ULP - BP20, FR-67037 Strasbourg Cedex, France*
[k] *Institute of Nuclear Physics, N.C.S.R. Demokritos, P.O. Box 60228, GR-15310 Athens, Greece*
[l] *FZU, Inst. of Phys. of the C.A.S. High Energy Physics Division, Na Slovance 2, CZ-180 40 Praha 8, Czech Republic*
[m] *Dipartimento di Fisica, Università di Genova and INFN, Via Dodecaneso 33, IT-16146 Genova, Italy*
[n] *Institut des Sciences Nucléaires, IN2P3-CNRS, Université de Grenoble 1, FR-38026 Grenoble Cedex, France*
[o] *Helsinki Institute of Physics, HIP, P.O. Box 9, FI-00014 Helsinki, Finland*
[p] *Joint Institute for Nuclear Research, Dubna, Head Post Office, P.O. Box 79, RU-101 000 Moscow, Russian Federation*
[q] *Institut für Experimentelle Kernphysik, Universität Karlsruhe, Postfach 6980, DE-76128 Karlsruhe, Germany*
[r] *Institute of Nuclear Physics and University of Mining and Metalurgy, Ul. Kawiory 26a, PL-30055 Krakow, Poland*
[s] *Université de Paris-Sud, Lab. de l'Accélérateur Linéaire, IN2P3-CNRS, Bât. 200, FR-91405 Orsay Cedex, France*
[t] *School of Physics and Chemistry, University of Lancaster, Lancaster LA1 4YB, UK*
[u] *LIP, IST, FCUL - Av. Elias Garcia, 14-1°, PT-1000 Lisboa Codex, Portugal*
[v] *Department of Physics, University of Liverpool, P.O. Box 147, Liverpool L69 3BX, UK*
[w] *LPNHE, IN2P3-CNRS, Univ. Paris VI et VII, Tour 33 (RdC), 4 place Jussieu, FR-75252 Paris Cedex 05, France*
[x] *Department of Physics, University of Lund, Sölvegatan 14, SE-223 63 Lund, Sweden*
[y] *Université Claude Bernard de Lyon, IPNL, IN2P3-CNRS, FR-69622 Villeurbanne Cedex, France*
[z] *Univ. d'Aix - Marseille II - CPP, IN2P3-CNRS, FR-13288 Marseille Cedex 09, France*
[aa] *Dipartimento di Fisica, Università di Milano and INFN, Via Celoria 16, IT-20133 Milan, Italy*
[ab] *Niels Bohr Institute, Blegdamsvej 17, DK-2100 Copenhagen Ø, Denmark*
[ac] *NC, Nuclear Centre of MFF, Charles University, Areal MFF, V Holesovickach 2, CZ-180 00 Praha 8, Czech Republic*
[ad] *NIKHEF, Postbus 41882, NL-1009 DB Amsterdam, The Netherlands*
[ae] *National Technical University, Physics Department, Zografou Campus, GR-15773 Athens, Greece*
[af] *Physics Department, University of Oslo, Blindern, NO-1000 Oslo 3, Norway*
[ag] *Dpto. Fisica, Univ. Oviedo, Avda. Calvo Sotelo s / n, ES-33007 Oviedo, Spain*
[ah] *Department of Physics, University of Oxford, Keble Road, Oxford OX1 3RH, UK*
[ai] *Dipartimento di Fisica, Università di Padova and INFN, Via Marzolo 8, IT-35131 Padua, Italy*
[aj] *Rutherford Appleton Laboratory, Chilton, Didcot OX11 OQX, UK*
[ak] *Dipartimento di Fisica, Università di Roma II and INFN, Tor Vergata, IT-00173 Rome, Italy*
[al] *Dipartimento di Fisica, Università di Roma III and INFN, Via della Vasca Navale 84, IT-00146 Rome, Italy*
[am] *DAPNIA / Service de Physique des Particules, CEA-Saclay, FR-91191 Gif-sur-Yvette Cedex, France*
[an] *Instituto de Fisica de Cantabria (CSIC-UC), Avda. los Castros s / n, ES-39006 Santander, Spain*
[ao] *Dipartimento di Fisica, Università degli Studi di Roma La Sapienza, Piazzale Aldo Moro 2, IT-00185 Rome, Italy*
[ap] *Inst. for High Energy Physics, Serpukov P.O. Box 35, Protvino (Moscow Region), Russian Federation*
[aq] *J. Stefan Institute, Jamova 39, SI-1000 Ljubljana, Slovenia and Department of Astroparticle Physics, School of Environmental Sciences, Kostanjeviska 16a, Nova Gorica, SI-5000 Slovenia, and Department of Physics, University of Ljubljana, SI-1000 Ljubljana, Slovenia*
[ar] *Fysikum, Stockholm University, Box 6730, SE-113 85 Stockholm, Sweden*
[as] *Dipartimento di Fisica Sperimentale, Università di Torino and INFN, Via P. Giuria 1, IT-10125 Turin, Italy*
[at] *Dipartimento di Fisica, Università di Trieste and INFN, Via A. Valerio 2, IT-34127 Trieste, Italy, and Istituto di Fisica, Università di Udine, IT-33100 Udine, Italy*
[au] *Univ. Federal do Rio de Janeiro, C.P. 68528 Cidade Univ., Ilha do Fundão, BR-21945-970 Rio de Janeiro, Brazil*
[av] *Department of Radiation Sciences, University of Uppsala, P.O. Box 535, SE-751 21 Uppsala, Sweden*
[aw] *IFIC, Valencia-CSIC, and D.F.A.M.N., U. de Valencia, Avda. Dr. Moliner 50, ES-46100 Burjassot (Valencia), Spain*
[ax] *Institut für Hochenergiephysik, Österr. Akad. d. Wissensch., Nikolsdorfergasse 18, AT-1050 Vienna, Austria*
[ay] *Inst. Nuclear Studies and University of Warsaw, Ul. Hoza 69, PL-00681 Warsaw, Poland*
[az] *Fachbereich Physik, University of Wuppertal, Postfach 100 127, DE-42097 Wuppertal, Germany*

Abstract

An update of the searches for charginos and neutralinos is presented, based on a data sample corresponding to the 53.9 pb^{-1} recorded by the DELPHI detector in 1997, at a centre-of-mass energy of 183 GeV. No evidence for a signal was found. The lower mass limits are 4–5 GeV/c^2 higher than those obtained at a centre-of-mass energy of 172 GeV. The (μ,M$_2$) domain excluded by combining the neutralino and chargino searches implies a limit on the mass of the lightest neutralino which, for a heavy sneutrino, is constrained to be above 29.1 GeV/c^2 for $\tan\beta \geq 1$. © 1999 Elsevier Science B.V. All rights reserved.

1. Introduction

In 1997, the LEP centre-of-mass energy reached 183 GeV, and the DELPHI experiment collected an integrated luminosity of 53.9 pb^{-1}. These data have been analysed to search for the supersymmetric partners of Higgs and gauge bosons, the charginos, neutralinos and gravitinos, predicted by supersymmetric (SUSY) models [1].

This paper presents an update of the results described in [2] which contains a detailed description of the analysis of $\sqrt{s}$ = 161–172 GeV data. The methods used to search for charginos and neutralinos presented in [2] have remained almost unchanged and only the differences from the previous analysis are described here. A description of the parts of the DELPHI detector relevant to the present paper can be found in [2], while the complete descriptions are given in [3].

It is assumed that R-parity is conserved, implying a stable lightest supersymmetric particle (LSP). As in the previous paper the two cases where either the lightest neutralino ($\tilde{\chi}_1^0$) or the gravitino ($\tilde{G}$) is the LSP are considered. In the former case, events are characterised by missing energy carried by the escaping neutralinos, while in the latter case the decay $\tilde{\chi}_1^0 \rightarrow \tilde{G}\gamma$ is possible [4–6]. If the gravitino is sufficiently light (with a mass below about 10 eV/c^2 [6]), this decay takes place within the detector. As gravitinos escape detection, the typical signature of these SUSY events is missing energy and isolated photons. The mass difference ΔM plays an impor-

tant role in the analysis, as the missing transverse momentum and visible mass depend strongly on this variable. ΔM is defined as the difference $M_{\mathrm{SUSY}} - M_{\tilde{\chi}_1^0}$ where M_{SUSY} is the mass of the particle searched for, the chargino or the neutralino.

The Minimal Supersymmetric Standard Model (MSSM) scheme with universal parameters at the high mass scale typical of Grand Unified Theories (GUTs) is assumed [1]. The parameters of this model relevant to the present searches are the masses M_1 and M_2 of the gaugino sector (which are assumed to satisfy the GUT relation $M_1 = \frac{5}{3}\tan^2\theta_W M_2 \approx 0.5 M_2$ at the electroweak scale), the universal mass m_0 of the scalar lepton sector, the Higgs mass parameter μ, and the ratio of vacuum expectation values of the two Higgs doublets, $\tan\beta$.

2. Data samples and event generators

The total integrated luminosity collected by DELPHI during 1997 at E_{cm} = 183 GeV was 53.9 pb^{-1}. This luminosity was used in the chargino analysis for topologies with a stable neutralino, while 50.6 pb^{-1} was used in topologies with an unstable neutralino due to a temporary problem in the read-out of the barrel electromagnetic calorimeter (HPC). The luminosity used in the neutralino analysis was 47.3 pb^{-1} due to different quality selection criteria.

To evaluate the signal efficiencies and background contaminations, events were generated using several different programs. All relied on JETSET 7.4 [7], tuned to LEP 1 data [8], for quark fragmentation.

The program SUSYGEN [9] was used to generate neutralino and chargino signal events in both the neutralino and gravitino LSP scenarios, and to calcu-

---

[1] On leave of absence from IHEP Serpukhov.
[2] Now at University of Florida.

late cross-sections and branching ratios. Details of these signal samples are given in Section 4.

The background process $e^+e^- \to q\bar{q}(n\gamma)$ was generated with PYTHIA 5.7 [7], while DYMU3 [10] and KORALZ [11] were used for $\mu^+\mu^-(\gamma)$ and $\tau^+\tau^-(\gamma)$, respectively. The generator of Ref. [12] was used for $e^+e^- \to e^+e^-$ events. Processes leading to four-fermion final states, $(Z/\gamma)^*(Z/\gamma)^*$, W^+W^-, $We\nu_e$ and Ze^+e^-, were also generated using PYTHIA. The calculation of the four-fermion background was verified using the program EXCAL-IBUR [13] which consistently takes into account all amplitudes leading to a given four-fermion final state, but does not include the transverse momentum of initial state radiation when electrons are present in the final state.

The VDM and QCD components of the two-photon interactions leading to hadronic final states were generated using TWOGAM [14]. The generators of Berends, Daverveldt and Kleiss [15] were used for the QPM component and for leptonic final states.

The generated signal and background events were passed through the detailed simulation of the DEL-PHI detector [3] and then processed with the same reconstruction and analysis programs as the real data. The numbers of simulated events from different background processes were several times the numbers in the real data.

3. Event selections

The criteria used to select events were defined on the basis of the simulated signal and background events. The selections for charged and neutral particles were the same as those presented in [2]. One new criterion was introduced in order to reject neutral clusters coming from the intrinsic radioactivity (mainly α) of the barrel electromagnetic calorimeter. Showers with less than 15 GeV of energy and with more than 90% of the energy deposited in one single calorimeter layer have been rejected. Fig. 1 shows the distribution of variables relevant for the selection of chargino topologies with a stable neutralino for real and simulated events. The agreement is satisfactory, the normalization is absolute.

As in [2], the particle selection was followed by different event selections in the different topologies.

Some of the selection criteria were slightly changed in order to maintain a good signal-to-background ratio. In fact the average value of some variables used to enhance the signal changed due to the increased $\sqrt{s}$.

One example is the missing transverse momentum for two-photon interactions which increases on average, while it doesn't change for a degenerate chargino close to the kinematic limit.

Other selection criteria were re-tuned due to the increased W^+W^- production cross-section (the criterion on the visible mass) or due to a better understanding of the signal. Some new analyses have been added in order to have a better efficiency for small values of ΔM. The differences in the selection criteria between the present analysis and the one at $\sqrt{s} = 161$ and 172 GeV [2] are in general quite small, apart from the addition of some new analyses, but are detailed below for completeness.

3.1. Chargino analysis

The remnants of the chargino decays were searched for in the following topologies: jets and one or more isolated charged lepton ($jj\ell$), jets only, purely leptonic final states ($\ell\ell$) and anything plus one or more isolated photons ($\gamma\gamma X$).

For the $jj\ell$ topology in the degenerate case ($\Delta M \leq 10\,\text{GeV}/c^2$), the minimal missing transverse momentum was changed from 3 to 4 GeV/c and a new requirement was introduced: the polar angles of both jet axes were required to be in the range $24° < \theta < 156°$.

For the jets topology in the non-degenerate case ($\Delta M > 10\,\text{GeV}/c^2$) the maximum allowed energy in the forward and backward 20° cones was changed from 30% of the visible energy to 50%, the maximum visible mass was changed to 65 GeV/c^2, and a new requirement of visible mass above 15 GeV/c^2 was added. In the degenerate case, the jet polar angles were required to be in the same range as in the $jj\ell$ topology.

For the $\ell\ell$ topology the different multiplicity-dependent criteria on the missing transverse momentum were changed to a single minimum value of 5.5 GeV/c for the non-degenerate case and 4 GeV/c for the degenerate case.

DELPHI, hadronic selection (183 GeV)

DELPHI, hadronic selection (183 GeV)

DELPHI, semileptonic selection (183 GeV)
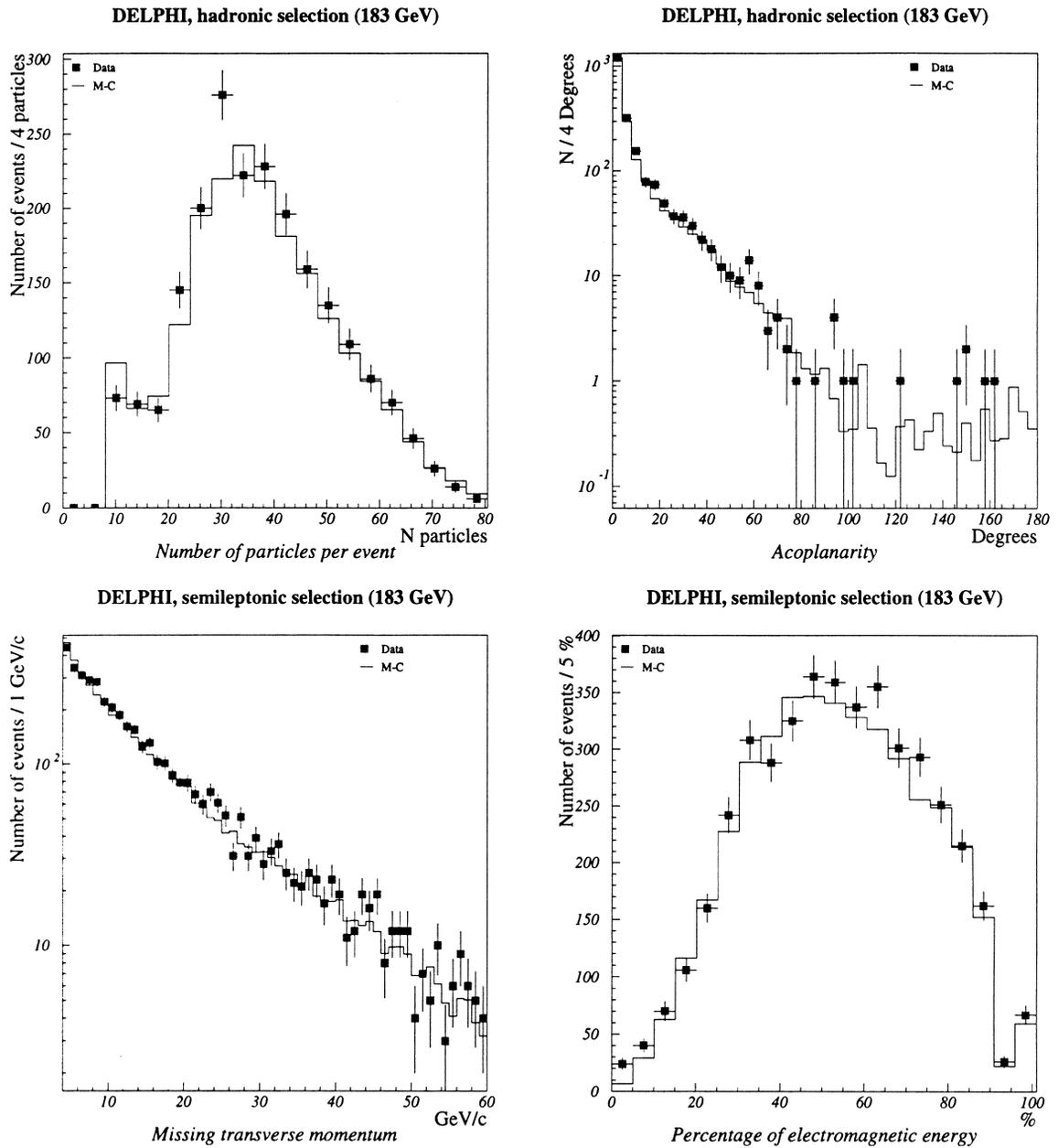
DELPHI, semileptonic selection (183 GeV)

Fig. 1. Distributions of total multiplicity and scaled acoplanarity after hadronic topology selection [2]. Distributions of missing transverse momentum and percentage of electromagnetic energy after the semileptonic topology selection [2]. *Points* show distributions for real data events, *histograms* for simulated events. The normalization of the histograms is absolute.

The selection criteria used in the gravitino LSP scenario are also used in the radiative topology ($\gamma\gamma$X) for the neutralino LSP scenario, when the cascade decay $\tilde{\chi}_i^{\pm} \rightarrow \tilde{\chi}_2^0 f\bar{f} \rightarrow \tilde{\chi}_1^0 \gamma f\bar{f}$ is possible for

low values of $\tan\beta$ and $M_2 \sim -\mu$. The requirement that the total visible mass should exceed 20 GeV/c^2 was added in the non-degenerate case. In the degenerate case (re-defined to be $5 \, \text{GeV}/c^2 < \Delta M \leq$

Table 1

The numbers of events observed in data and the expected numbers of background events in the different chargino search channels under the hypothesis of a stable neutralino (Section 3.1)

	Chargino channels (stable neutralino)						
	Non-degenerate case			Degenerate case			
topology:	$jj\ell$	jets	$\ell\ell$	$\gamma\gamma$X	$jj\ell$	jets	$\ell\ell$
obs. events:	0	11	7	3	4	3	1
background:	1.0 ± 0.8	7.6 ± 0.9	8.8 ± 1.0	4.9 ± 0.8	3.3 ± 0.9	5.1 ± 0.9	1.9 ± 0.8
total:							
obs. events:		21				8	
background:		22.3 ± 1.8				10.3 ± 1.1	

$10\,\mathrm{GeV}/c^2$), the minimum scaled acoplanarity [2] was changed from $5°$ to $10°$ and the momentum of the most energetic charged particle was required not to exceed $15\,\mathrm{GeV}/c$, rather than $30\,\mathrm{GeV}/c$. A *new selection for the ultra-degenerate case* [16] was introduced to increase the signal efficiency for $\Delta M \leq 5\,\mathrm{GeV}/c^2$. In this case, the energy of the most energetic isolated photon had to lie between 20 GeV and 60 GeV, and the momentum of the most energetic charged particle was required to be smaller than 10 GeV/c. The visible mass of the event, excluding the isolated photons, had to be smaller than $40\,\mathrm{GeV}/c^2$, and the scaled acoplanarity greater than $5°$. Finally, the same criteria as in the degenerate case were applied to the missing transverse momentum, to the percentage of energy in the forward and backward $25°$ cones and to the total electromagnetic energy, excluding the energy of the most energetic isolated photon.

3.2. Neutralino analysis

Neutralino final states were searched for in purely hadronic and purely leptonic topologies.

A new criterion on the charged multiplicity was added in the selection of the jj topology: at least four well reconstructed charged particles, including one with a transverse momentum exceeding $1\,\mathrm{GeV}/c$, were required. Other new selection criteria were added: the sum of the absolute values of the momenta of well reconstructed charged particles had to be greater than $4\,\mathrm{GeV}/c$; the transverse energy of the event was required to be greater than 4 GeV; no charged particle was allowed to have a momentum

greater than 20 GeV/c; and finally, the most isolated identified electron or muon with an isolation angle to the nearest jet greater than $20°$was required to have momentum less than $10\,\mathrm{GeV}/c$. The maximum allowed fraction of the total energy of particles emitted within $30°$ of the beam was changed from 40% to 60%. The last step in the selection consisted of the logical OR of three sets of cuts, optimised for different regions of ΔM:

· For low ΔM ($\sim 10\,\mathrm{GeV}/c^2$), minimum requirements on the scaled acoplanarity ($40°$) and on the missing transverse momentum ($7.0\,\mathrm{GeV}/c$) were added.

· For intermediate ΔM ($\sim 40\,\mathrm{GeV}/c^2$), the selection criteria on the multiplicity, on the total energy in the forward and backward $30°$ cones, and on the polar angle of the missing momentum were removed. The invariant mass range of visible particles was required to be between $0.1\sqrt{s}\,/c^2$ and $0.3\sqrt{s}\,/c^2$, the minimum missing mass value was changed from $0.5\sqrt{s}\,/c^2$ to $0.6\sqrt{s}\,/c^2$.

· For large ΔM ($\sim 90\,\mathrm{GeV}/c^2$) all selection criteria are new: the invariant mass of visible particles was required to be greater than 0.3 and less than

Table 2

The numbers of events observed in data and the expected numbers of background events in the different neutralino search channels (Section 3.2)

	Neutralino channels	
topology:	jj	$\ell\ell$
obs. events:	6	5
background:	8.2 ± 1.2	6.9 ± 0.6

$0.5\sqrt{s}/c^2$, and the missing mass had to exceed $0.45\sqrt{s}/c^2$. The scaled acoplanarity had to exceed 25° and the missing transverse momentum had to exceed 8 GeV/c and be less than 35 GeV/c. It was also required that the component of the missing momentum in the beam direction should be less than 35 GeV/c.

The analysis which selected neutralino decays giving di-leptons ($\ell\ell$) was re-optimised to cope with the increased W^+W^- background and its different kinematic characteristics. This analysis selected events with exactly two isolated, oppositely charged particles reconstructed with momenta above 1 GeV/c where the isolation criteria requires that there should be no more than 2 GeV of charged energy in a 10° cone around the track. The total multiplicity of the event should not exceed five. It was also required that both selected tracks should have hits in at least four pad rows in the Time Projection Chamber and with at least one associated hit in the vertex detector. Finally, either both particles had to be identified as electrons or muons (*loose tag* [17]), or one of them had to satisfy stricter electron identification criteria (*standard tag*). To reject $e^+e^- \rightarrow e^+e^-$ and $Z\gamma$ events, the acoplanarity between the two selected particles was required to exceed 10°. Events produced in two-photon interactions were rejected by demanding that the direction of the missing momentum satisfy $|\cos\theta_{p_{\text{miss}}}| < 0.9$, and that its transverse component be greater than 5 GeV/c. It was also required that the energy in the 30° cone around the beam be less than 70% of the visible energy, that no neutral cluster with energy above 15 GeV and no more than 1 GeV of energy was detected in the very forward and backward electromagnetic calorimeter (STIC). To reduce the number of events from leptonic decays of W^+W^- pairs, events were rejected if one particle
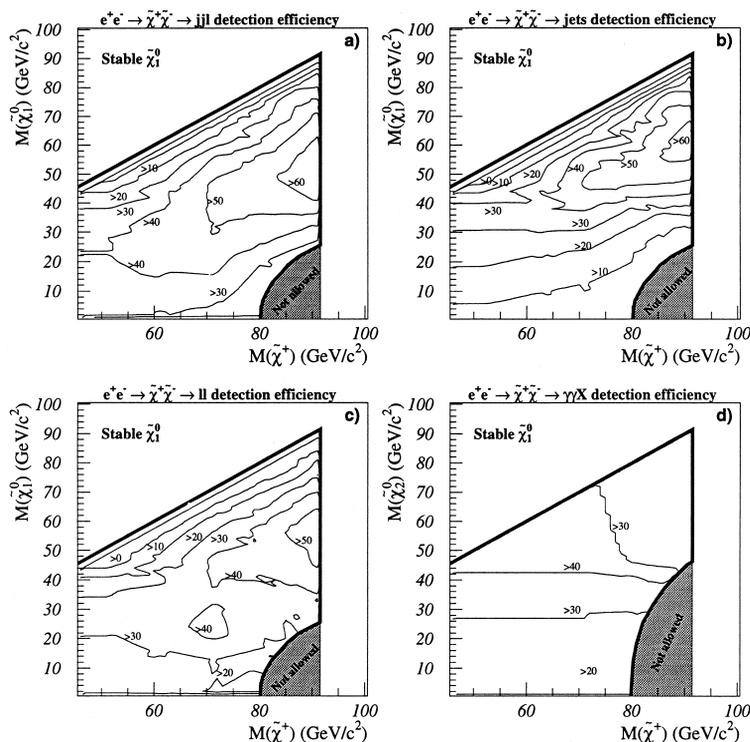

Fig. 2. Chargino pair production detection efficiencies (%) for the 4 topologies a) $jj\ell$, b) jets, c) $\ell\ell$ and d) $\gamma\gamma$X, at 183 GeV in the $(M_{\tilde{\chi}^\pm}, M_{\tilde{\chi}^0})$ plane. A stable neutralino is assumed.

was identified (*loose tag*) as an electron and the other as a muon. In a similar manner as in the *jj* topology the different regions of ΔM were selected:

· Low ΔM (~ 10 GeV/c^2): the invariant mass of visible particles was required to be less than $0.1\sqrt{s}$ /c^2, the missing mass had to exceed $0.7\sqrt{s}$ /c^2, the acoplanarity had to exceed $40°$ and the missing transverse momentum had to exceed 8.0 GeV/c.

· Intermediate ΔM (~ 40 GeV/c^2): the invariant mass of visible particles was required to be between $0.1\sqrt{s}$ /c^2 and $0.3\sqrt{s}$ /c^2, and the missing mass had to exceed $0.45\sqrt{s}$ /c^2. The acoplanarity had to exceed $25°$ and the missing transverse momentum had to exceed 10 GeV/c.

· Large ΔM (~ 90 GeV/c^2): the invariant mass of visible particles was required to be between $0.3\sqrt{s}$ /c^2 and $0.55\sqrt{s}$ /c^2, and the missing mass had to exceed $0.4\sqrt{s}$ /c^2. The acoplanarity had to

exceed $15°$ and the missing transverse momentum had to exceed 12 GeV/c.

4. Results in case of a stable neutralino

4.1. Efficiencies and selected events

The total number of background events expected in the different topologies is shown in Tables 1 and 2, together with the number of events selected in the data.

The efficiencies of the chargino selections in Section 3.1 were estimated using 37 combinations of $\tilde{\chi}_1^{\pm}$ and $\tilde{\chi}_1^0$ masses in four chargino mass ranges ($M_{\tilde{\chi}_1^{\pm}} \approx 91$, 85, 70 and 50 GeV/$c^2$) and with ΔM ranging from 1 GeV/c^2 to 70 GeV/c^2. A total of 74000 chargino events was generated and passed through the complete simulation of the DELPHI detector. A special study was carried out in the
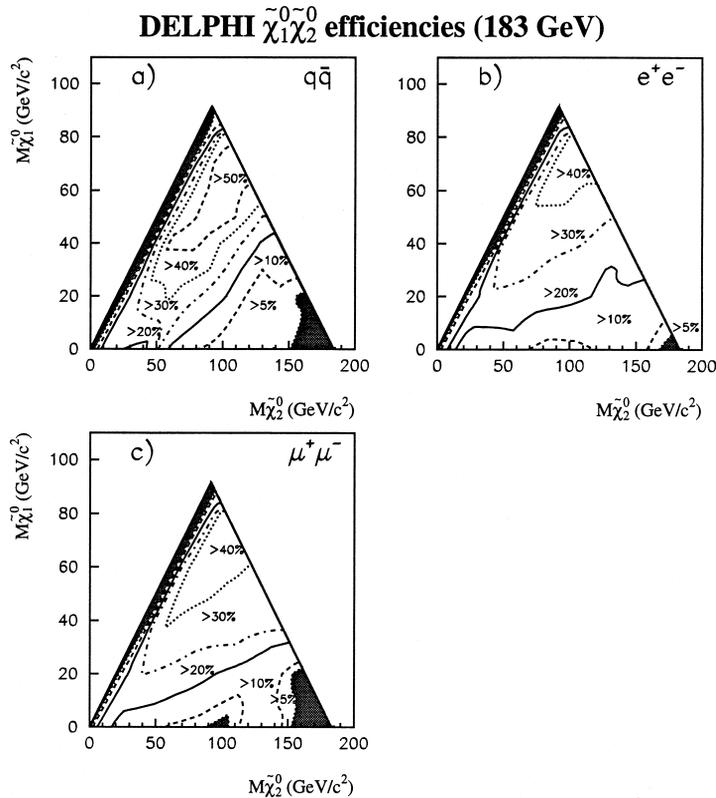

Fig. 3. Neutralino pair production detection efficiency for the *jj*, e$^+$e$^-$ and $\mu^+\mu^-$ topologies at 183 GeV in the ($M_{\tilde{\chi}_2^0}, M_{\tilde{\chi}_1^0}$) plane. The shaded areas are regions where the efficiency is lower than 5%.

region of low $|\mu|$ and M_2 as described in [2]. The efficiencies for the four different topologies are shown in Fig. 2. For the $\gamma\gamma X$ topology, the efficiency depends mainly on $\Delta M = M_{\tilde{\chi}^\pm} - M_{\tilde{\chi}^0_2}$ and is practically independent of the photon energy.

For the neutralino analysis, a total of 130000 $\tilde{\chi}^0_1\tilde{\chi}^0_2$ events was generated for 42 different combinations of $M_{\tilde{\chi}^0_2}$ and $M_{\tilde{\chi}^0_1}$ masses with $M_{\tilde{\chi}^0_1}$ ranging from 10 GeV/c^2 to 85 GeV/c^2, with $M_{\tilde{\chi}^0_2} - M_{\tilde{\chi}^0_1}$ ranging from 5 GeV/c^2 to the kinematic limit, and for different $\tilde{\chi}^0_2$ decay modes ($q\bar{q}\,\tilde{\chi}^0_1$, $\mu^+\mu^-\tilde{\chi}^0_1$, $e^+e^-\tilde{\chi}^0_1$). The efficiencies for the neutralino selections in Section 3.2 are shown in Fig. 3.

The numbers of selected events are compatible with the expectation from the background simulation in all the channels considered. As no evidence for a signal is found, exclusion limits are set.

4.2. Limits

4.2.1. Limits on neutralino production

Limits on neutralino production in the case of a stable $\tilde{\chi}^0_1$ were derived from the parametrized efficiencies of Section 3.2 and the observed numbers of events, as described in [2]. The limits obtained for the $\tilde{\chi}^0_1\tilde{\chi}^0_2$ production cross-section are shown in Figs. 4a,b and c assuming 100% branching ratio for the hadronic or leptonic decay modes. The limit obtained assuming that the $\tilde{\chi}^0_2 \rightarrow \tilde{\chi}^0_1 f\bar{f}$ decay is mediated by a Z^*, including both leptonic and hadronic modes and 20% of invisible final states, is of about 1 pb as seen in Fig. 4d. These limits also apply to $\tilde{\chi}^0_1\tilde{\chi}^0_k$ ($k = 3,4$) production with $\tilde{\chi}^0_k$ decaying into $\tilde{\chi}^0_1$.
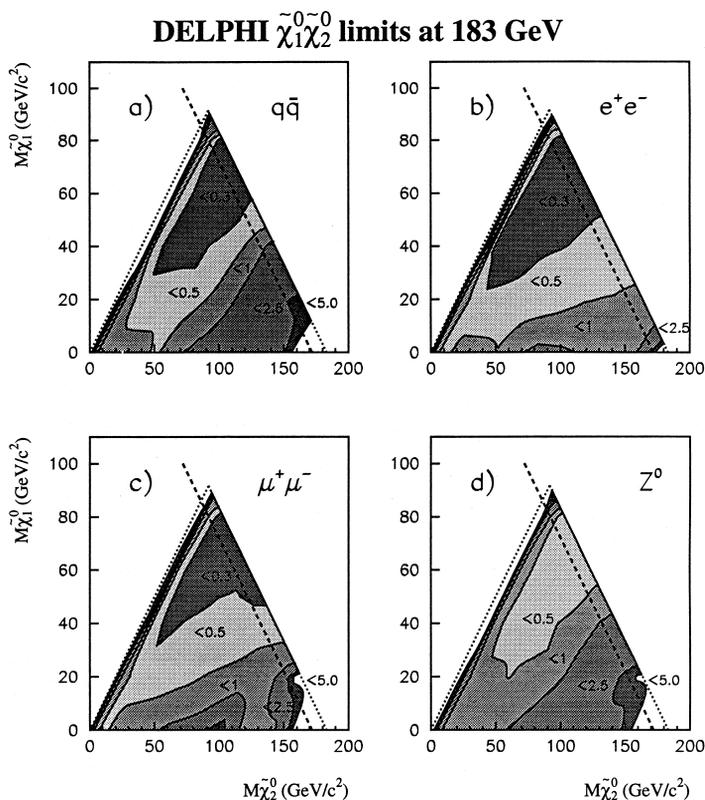

Fig. 4. Contour plots of upper limits on the cross-sections at the 95% confidence level for $\tilde{\chi}^0_1\tilde{\chi}^0_2$ production at $\sqrt{s}$ = 183 GeV. In each plot, the different shades correspond to regions where the cross-section limit in picobarns is below the indicated number. For figures a), b), c), $\tilde{\chi}^0_2$ decays into $\tilde{\chi}^0_1 q\bar{q}$, $\tilde{\chi}^0_1 e^+e^-$, and $\tilde{\chi}^0_1 \mu^+\mu^-$, respectively, were assumed to dominate. In d), the $\tilde{\chi}^0_2$ was assumed to decay into $\tilde{\chi}^0_1 f\bar{f}$ with the same branching ratios into different fermion flavours as the Z. The dotted lines indicate the kinematic limit and the defining relation $M_{\tilde{\chi}^0_2} > M_{\tilde{\chi}^0_1}$, and the dashed lines indicate the kinematic limit of the search at 172 GeV [2].

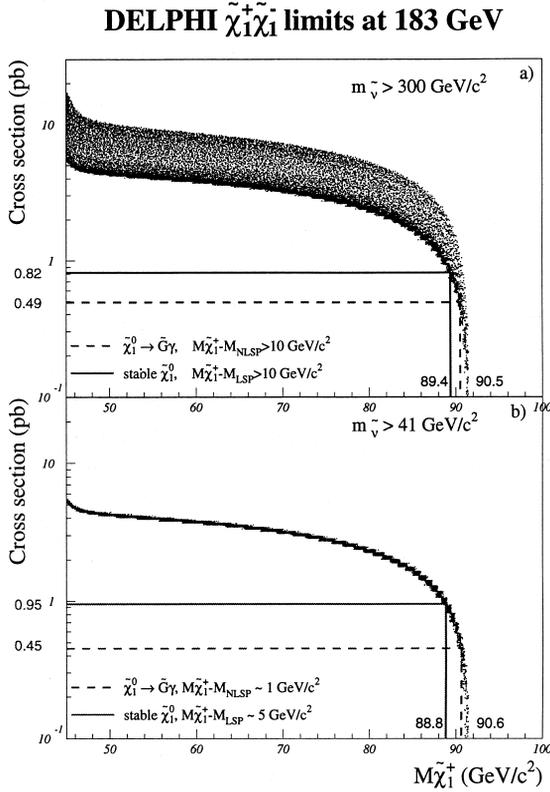## DELPHI $\tilde{\chi}_1^+\tilde{\chi}_1^-$ limits at 183 GeV

Fig. 5. Expected cross-sections in pb at 183 GeV (dots) versus the chargino mass in a) in the non-degenerate case ($\Delta M > 10$ GeV/c^2) and in b) in the degenerate case ($\Delta M \leq 5$ GeV/c^2). The spread in the dots originates from the random scan over the parameters μ and M_2. A heavy sneutrino ($m_{\tilde{\nu}} > 300$ GeV/c^2) has been assumed in a) and $m_{\tilde{\nu}} > 41$ GeV/c^2 in b). The 95% C.L. limits on the cross-sections corresponding to the mass limits are indicated by the horizontal lines.

4.2.2. Limits on chargino production

The simulated data points were used to parametrize the efficiencies of the chargino selection criteria described in Section 3.1 in terms of ΔM and the mass of the chargino. Then a large number of SUSY points were investigated and the values of ΔM, the chargino and neutralino masses and the various decay branching ratios were determined for each point. By applying the appropriate efficiency and branching ratios for each channel the number of expected signal events for a given cross-section can be calculated. Taking also the expected background and the number of events actually observed into account, certain cross-sections, or the corresponding

points in the MSSM parameter space (μ, M_2, $\tan\beta$), may be excluded.

Fig. 5 shows the chargino production cross-sections obtained in the MSSM at $\sqrt{s} = 183$ GeV for different chargino masses for the non-degenerate and degenerate cases. The parameters M_2 and μ were varied randomly in the ranges 0 GeV/c^2 < M_2 < 3000 GeV/c^2 and -400 GeV/c^2 < μ < 400 GeV/c^2 for three different values of $\tan\beta$, namely 1, 1.5 and 35. Two different cases were considered for the sneutrino mass: $M_{\tilde{\nu}} > 300$ GeV/c^2 (in the non-degenerate case) and $M_{\tilde{\nu}} > 41$ GeV/c^2 (in the degenerate case).

Applying the appropriate efficiencies and branching ratios for each of the points shown, the minimum non-excluded $M_{\tilde{\chi}_1^\pm}$ was determined. In the derivation of the chargino mass limits, constraints on the process $Z \to \tilde{\chi}_1^0 \tilde{\chi}_2^0 \to \tilde{\chi}_1^0 \tilde{\chi}_1^0 \gamma$ were also included. These were derived from the DELPHI results on single-photon production at LEP 1 [18]. The chargino mass limits are summarized in Table 3. The table also gives, for each case, the minimum excluded MSSM cross-section corresponding to the limit on the chargino mass. These cross-section values are also displayed in Fig. 5.

In the non-degenerate case with a large sneutrino mass (> 300 GeV/c^2), the lower limit for the chargino ranges between 89.4 GeV/c^2 (for a mostly higgsino-like chargino) and 90.8 GeV/c^2 (for a mostly wino-like chargino). The minimum excluded MSSM cross-section at $\sqrt{s} = 183$ GeV is 0.82 pb, corresponding to the limit on the chargino mass.

Table 3
95% confidence level limits for the chargino mass, the corresponding pair production cross-sections at 183 GeV and the 95% confidence level upper limit on the number of observed events, for the non-degenerate case and for a highly degenerate case. The scenarios of a stable $\tilde{\chi}_1^0$ and $\tilde{\chi}_1^0 \to \tilde{G}\gamma$ are considered

Case	$m_{\tilde{\nu}}$ (GeV/c^2)	$M_{\chi^\pm}^{\text{excl}}$ (GeV/c^2)	σ^{excl} (pb)	$N_{95\%}$
stable neutralino				
$\Delta M > 10$ GeV/c^2	> 300	89.4	0.82	10.14
$\Delta M = 5$ GeV/c^2	> 41	88.8	0.95	6.39
unstable neutralino				
$\Delta M > 10$ GeV/c^2	> 300	90.5	0.49	4.69
$\Delta M = 1$ GeV/c^2	> 41	90.6	0.45	4.36

In the degenerate case ($\Delta M = 5$ GeV/c^2), the cross-section does not depend significantly on the sneutrino mass, since the chargino is higgsino-like under the assumption of gaugino mass unification. The lower limit for the chargino mass, shown in Fig. 5, is 88.8 GeV/c^2. The minimum excluded MSSM cross-section is in this case 0.95 pb.

4.2.3. Limits on MSSM parameters and neutralino mass

Using the limits on chargino production and on LEP 1 single-photon production the excluded region in the plane of neutralino mass versus chargino mass was determined, as shown in Fig. 6. A heavy sneutrino was assumed. The small region outside the chargino kinematic limit derives from the single-photon search.

The exclusion regions in the (μ, M_2) plane are shown in Fig. 7 for different values of $\tan\beta$, assuming a heavy sneutrino and a heavy selectron ($m_0 = 1$ TeV/c^2). When different event selections contributed to the same physical production channel the efficiency and background of a logical OR of the channels was used, otherwise the method of Ref. [19] was used to combine the selections. These limits, based on data taken at $\sqrt{s} = 183$ GeV, improve on previous limits at lower energies, and represent a significant increase in range as compared to LEP 1 results [20]. The neutralino analysis independently excludes a substantial part of the region covered by the chargino search, and marginally extends this region at low $\tan\beta$ for large M_2 and negative μ.

Under the assumption that $M_1/M_2 \gtrsim 0.5$, the exclusion regions in the (μ, M_2) plane can be translated into the limit on the mass of the lightest
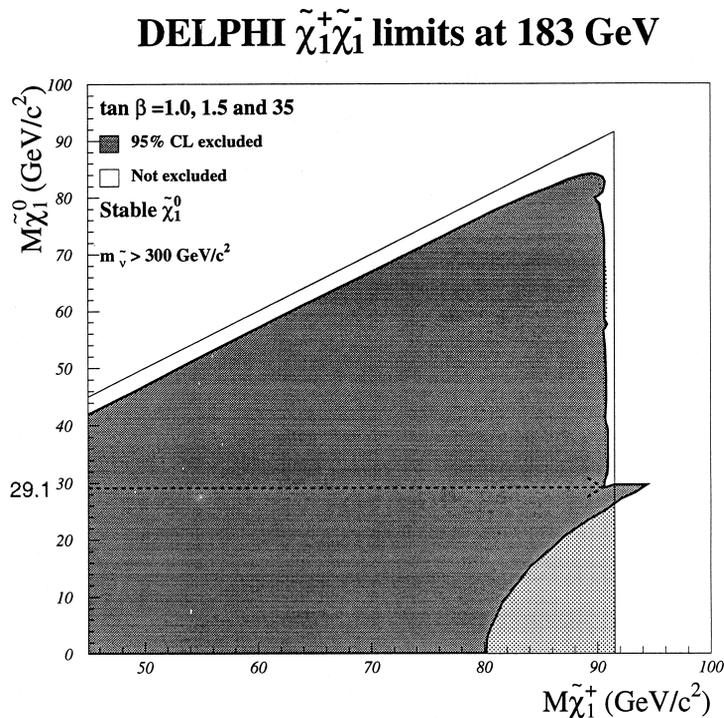

Fig. 6. Region excluded at 95% confidence level in the plane of the mass of the lightest neutralino versus that of the lightest chargino under the assumption of a heavy sneutrino, for $\tan\beta = 1.0$, 1.5 and 35. The thin lines show the kinematic limits in the production and the decay. The dotted line (sometimes hidden under the real exclusion limit) shows the expected exclusion limit. The lightly shaded region is not allowed in the MSSM. The limit applies in the case of a stable neutralino. The mass limit on the lightest neutralino is indicated by the horizontal dashed line. The excluded region outside the kinematic limit is obtained from the limit on $\tilde{\chi}_1^0 \tilde{\chi}_2^0$ production at the Z resonance derived from the single-photon search.
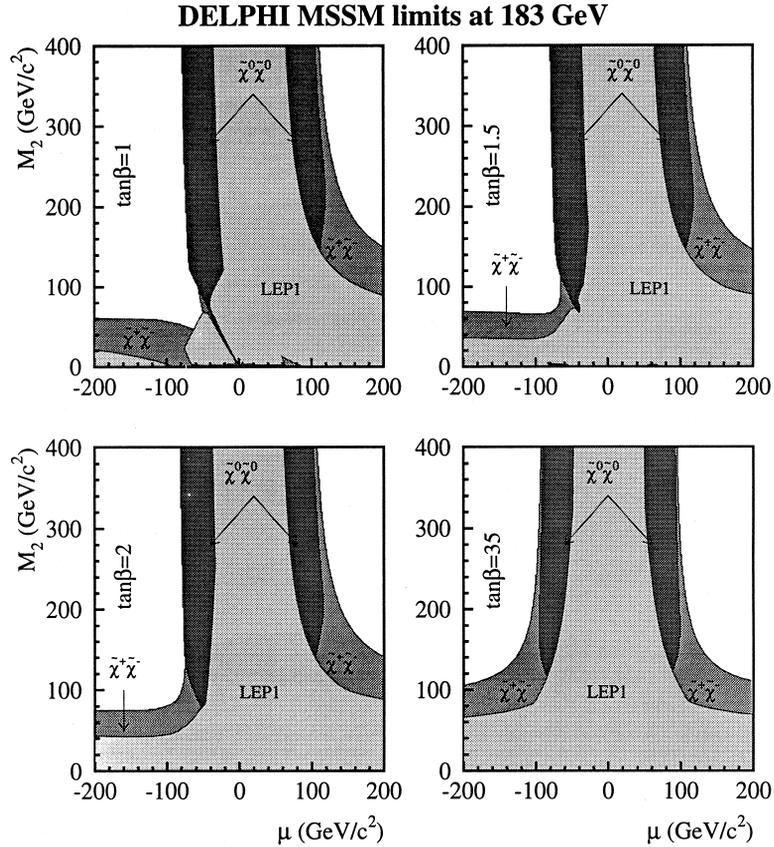
DELPHI MSSM limits at 183 GeV

Fig. 7. Regions in the (μ, M_2) plane excluded at 95% confidence level for different values of $\tan\beta$, assuming $m_0 = 1$ TeV/c^2. The lightly shaded areas are those excluded by lower energy LEP 1 results [20]. The intermediate shading shows regions excluded by the chargino search at 183 GeV. The dark shaded areas show the regions excluded by the neutralino search at these energies. With the exception of a narrow strip at negative μ for $\tan\beta \sim 1$ the regions excluded by the neutralino results are also excluded by the chargino search.

neutralino shown in Fig. 6. A lower limit of 29.1 GeV/c^2 on the lightest neutralino mass is obtained, valid for $\tan\beta \geq 1$, using the obtained chargino exclusion regions and including the DELPHI results [18] on the process $Z \to \tilde{\chi}_1^0 \tilde{\chi}_2^0 \to \tilde{\chi}_1^0 \tilde{\chi}_1^0 \gamma$. The lower mass limit is obtained for $\tan\beta = 1$, $\mu = -62.3$ GeV/c^2, $M_2 = 46.0$ GeV/c^2.

5. Results in case of an unstable neutralino

5.1. Efficiencies and selected events

The efficiency of the chargino selection for an unstable neutralino decaying into a photon and a

gravitino was calculated from a total of 78000 events generated using the same combinations of $M_{\tilde{\chi}_1^\pm}$ and $M_{\tilde{\chi}_1^0}$ as in the stable neutralino scenario. As mentioned in [2], the same selection applies to all topologies. The efficiency, shown in Fig. 8, varies only weakly with ΔM and is around 50%. Note that, due to the presence of the photons from the neutralino decay, the region of high degeneracy (down to $\Delta M = 1$ GeV/c^2) is fully covered.

The total number of background events expected in the different ΔM ranges is shown in Table 4, together with the number of events selected in the data. 4 events were found in the data, with a total expected background of 6.3 ± 0.9. The 3 events

DELPHI $\tilde{\chi}^+\tilde{\chi}^-$ efficiencies (183 GeV)

Total detection efficiency
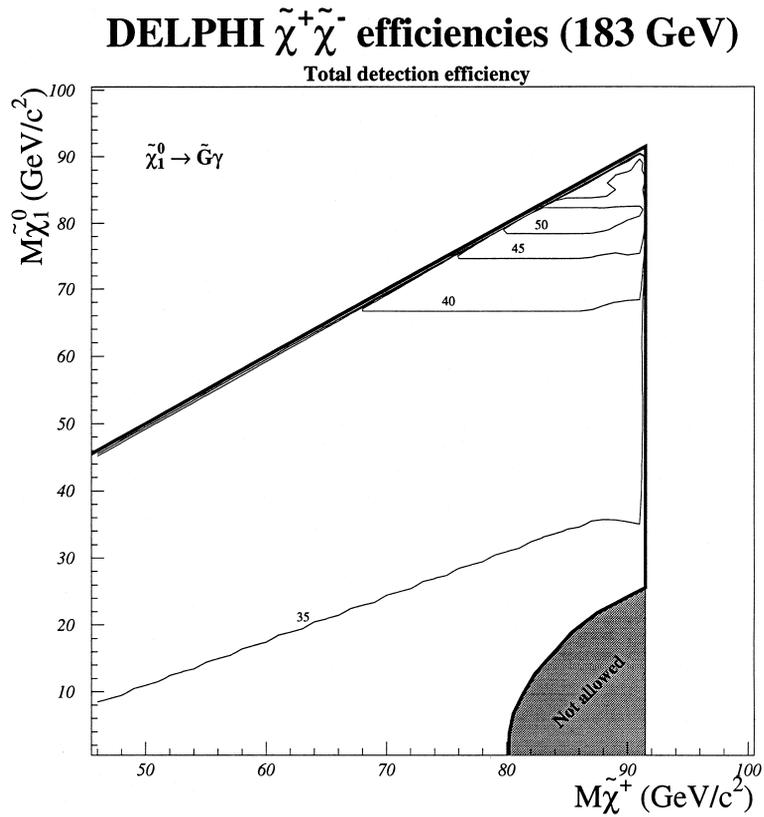
$\tilde{\chi}_1^0 \to \tilde{G}\gamma$

Fig. 8. Chargino pair production detection efficiency (%) at 183 GeV in the $(M_{\tilde{\chi}^\pm}, M_{\tilde{\chi}^0})$ plane. An unstable neutralino is assumed.

selected in the non-degenerate case are the same as the ones selected in the chargino $\gamma\gamma X$ topology in case of a stable neutralino. No signal is found, and exclusion limits have been set.

5.2. Limits

The chargino cross-section limits corresponding to the case where the neutralino is unstable and decays to $\tilde{G}\gamma$ have been computed as explained in Section 4.2 and are shown in Fig. 5 and in Table 3. In the non-degenerate case the chargino mass limit at 95% confidence level is 90.5 GeV/c^2 for a heavy sneutrino, while in the ultra-degenerate case ($\Delta M = 1$ GeV/c^2) the limit is 90.6 GeV/c^2. The minimum MSSM cross-section excluded by the above mass limits are 0.49 pb in the non-degenerate case and 0.45 pb in the ultra-degenerate case.

Table 4

The number of events observed and the expected number of background events in the different ΔM cases under the hypothesis of an unstable neutralino (Section 3.1)

	Chargino channels (unstable neutralino)		
	non-degenerate selection	degenerate selection	ultra-degenerate selection
Obs. events:	3	0	1
Background:	4.9 ± 0.8	0.9 ± 0.3	0.5 ± 0.2

6. Summary

Searches for charginos and neutralinos at $\sqrt{s} = 183$ GeV allow the exclusion of a large domain of SUSY parameters (at the 95% confidence level).

Assuming a difference in mass between chargino and neutralino, ΔM, of 10 GeV/c^2 or more, and a sneutrino heavier than 300 GeV/c^2, the existence of a chargino lighter than 89.4 GeV/c^2 is excluded. If a gaugino-dominated chargino is assumed in addition, the mass is above 90.8 GeV/c^2. If ΔM is between 5 GeV/c^2 and 10 GeV/c^2, the lower limit on the chargino mass becomes 88.8 GeV/c^2, independent of the sneutrino mass.

Limits on the cross-section for $\tilde{\chi}_1^0 \tilde{\chi}_2^0$ production of about 1 pb are obtained, and the excluded region in the (μ, M_2) plane is extended by the combined use of the neutralino and chargino searches. A special study of the low $|\mu|$, M_2, $\tan\beta$ region gives a limit on the mass of the lightest neutralino, valid in the case of large m_0, of 29.1 GeV/c^2.

The search for $\tilde{\chi}_1^+ \tilde{\chi}_1^-$, assuming the lightest neutralino decayed into photon and gravitino, gave somewhat more stringent limits on cross-sections and masses than in the case of a stable $\tilde{\chi}_1^0$: 90.5 GeV/c^2 for large ΔM and 90.6 GeV/c^2 for $\Delta M = 1$ GeV/c^2.

Acknowledgements

References

[1] P. Fayet, S. Ferrara, Phys. Rev. D 32 (1977) 249; H.P. Nilles, Phys. Rev. D 110 (1984) 1; H.E. Haber, G.L. Kane, Phys. Rev. D 117 (1985) 75.

[2] DELPHI Collaboration, P. Abreu et al., Eur. Phys. J. C 1 (1998) 1.

[3] DELPHI Collaboration, P. Aarnio et al., Nucl. Instr. and Meth. 303 (1991) 233.

[4] D. Dicus et al., Phys. Rev. D 41 (1990) 2347; D 43 (1991) 2951; Phys. Lett. B 258 (1991) 231.

[5] S. Dimopoulos et al., Phys. Rev. Lett. 76 (1996) 3494; S. Ambrosanio et al., Phys. Rev. Lett. 76 (1996) 3498; J.L. Lopez, D.V. Nanopoulos, Mod. Phys. Lett. A 10 (1996) 2473; D 55 (1997) 4450.

[6] S. Ambrosanio, Phys. Rev. D 54 (1996) 5395.

[7] T. Sjöstrand, Comp. Phys. Comm. 39 (1986) 347; T. Sjöstrand, PYTHIA 5.6 and JETSET 7.3, CERN-TH/6488-92.

[8] DELPHI Collaboration, P. Abreu et al., Z. Phys. C 73 (1996) 11.

[9] S. Katsanevas, P. Morawitz, IC/HEP/97-5, IFAE-UAB/97-01, LYCEN 9744, hep-ph/9711417.

[10] J.E. Campagne, R. Zitoun, Z. Phys. C 43 (1989) 469.

[11] S. Jadach, Z. Was, Comp. Phys. Comm. 79 (1994) 503.

[12] F.A. Berends, R. Kleiss, W. Hollik, Nucl. Phys. B 304 (1988) 712.

[13] F.A. Berends, R. Pittau, R. Kleiss, Comp. Phys. Comm. 85 (1995) 437.

[14] S. Nova, A. Olshevski, T. Todorov, in CERN Report 96-01, vol. 2, p. 224.

[15] F.A. Berends, P.H. Daverveldt, R. Kleiss, Comp. Phys. Comm. 40 (1986) 271, 285, 309.

[16] I. Gil, S. Navas, P. Rebecchi, Review of the chargino and gravitino search in DELPHI. Latest results at $E_{cm} = 183$ GeV, DELPHI note 98-56 MORIO CONF 129.

[17] DELPHI Collaboration, P. Abreu et al., Nucl. Instr. and Meth. 378 (1996) 57.

[18] DELPHI Collaboration, P. Abreu et al., Z. Phys. C 74 (1997) 577.

[19] V.F. Obraztsov, Nucl. Instr. and Meth. 316 (1992) 388.

[20] ALEPH Collaboration, D. Decamp et al., Phys. Rev. D 216 (1992) 253; A. Lopez-Fernandez, DELPHI note 92-95 (Dallas) PHYS 206; L3 Collaboration, M. Acciarri et al., Phys. Lett. B 350 (1995) 109; OPAL Collaboration, G. Alexander et al., Phys. Lett. B 377 (1996) 273.